

H₂, HD, and D₂ abundances on ice-covered dust grains in dark clouds

L. E. Kristensen^{1,*}, L. Amiaud^{2,3}, J.-H. Fillion^{4,5}, F. Dulieu¹, and J.-L. Lemaire¹

¹ LAMAp/LERMA, UMR8112 du CNRS, de l'Observatoire de Paris et de l'Université de Cergy Pontoise, 5 mail Gay-Lussac, 95000 Cergy Pontoise Cedex, France

e-mail: jean-louis.lemaire@obspm.fr

² Univ. Paris-Sud, ISMO, UMR 8214, 91405 Orsay, France

³ CNRS, UMR 8214, ISMO, 91405 Orsay, France

⁴ UPMC Univ. Paris 6, UMR 7092, LPMAA, 75005 Paris, France

⁵ CNRS, UMR 7092, LPMAA, 75005 Paris, France

Received 20 March 2009 / Accepted 21 December 2010

ABSTRACT

Aims. We seek to study the abundances of H₂, HD, and D₂ adsorbed onto ice-covered dust grains in dark molecular clouds in the interstellar medium.

Methods. We use our previously developed detailed model describing temperature-programmed desorption (TPD) experiments of H₂ and its isotopologues on water ice. We here extrapolate these model results from laboratory conditions to conditions similar to those found in dark molecular clouds.

Results. By means of our model we are able to infer three important results. (i) The time scale for H₂ and isotopologues to accrete onto dust grains is less than 10⁴ yrs. (ii) Due to the higher binding energy of D₂ with respect to HD, D₂ becomes the most abundant deuterated species on grains by ~50% with respect to HD (a few times 10⁻⁵ with respect to H₂). (iii) The surface coverage of D₂ as a function of temperature shows that at very low temperatures (i.e., less than 10 K), D₂ may be two orders of magnitude more abundant than HD. Possible implications for deuteration of water on grain surfaces are discussed when it forms through reactions between OH and H₂.

Key words. ISM: molecules – molecular processes – astrochemistry

1. Introduction

In cold dark molecular clouds, the main gas components are molecular hydrogen (H₂) and helium, accounting for 90% and 10% of the total number density, respectively. These are the main gas components by ~four orders of magnitude. When it comes to mass, H₂ and He still are the principal components (~74% and ~25%, respectively), but another component is the interstellar dust (~1%). In dark clouds, the temperature is typically ≤10–15 K, the density is ~10⁴–10⁵ cm⁻³, and it is expected most heavier species will have frozen out onto the dust grain surfaces where they form a thick layer of molecular ice, the principal ice component being water (Gibb et al. 2004).

Most of the theoretical and experimental work on H₂ ice surface chemistry has so far focused on H₂ formation (through the H + H → H₂ surface reaction) in terms of the efficiency and the energy budget (e.g. Govers et al. 1980; Congiu et al. 2009), and the role of the substrate in the formation process has also been studied (Hornekær et al. 2003, 2005). The main reason for this is that it is assumed H₂ does not freeze out onto dust grains as the sublimation temperature is ~4 K (Sandford et al. 1993; Buch & Devlin 1994; Dissly et al. 1994). However, the amount of gas phase H₂ is so overwhelming that grain-H₂ collisions are inevitable at all temperatures found in a cold dark cloud. Moreover, icy grain mantles are believed to be amorphous

in nature, and their corrugated surface might have a large surface area. This means that the presence of molecular hydrogen on the surface of icy grain mantles should be considered in detail in the context of surface chemistry.

If non-negligible amounts of H₂ are present on the grain surface, the chemistry could be affected. In particular, any barrierless reactions involving H₂ could be enhanced on the surface, with the formation of water being one such example. It is suggested by Tielens et al. (1983) that the following reaction may take place on dust grain surfaces:



This reaction has been studied theoretically alongside several others reaction paths, and is found to be the most efficient path under cold, dark-cloud conditions (Cuppen & Herbst 2007). One of the key questions for this route to be active in such regions is, how much H₂ is available on the surface? As a side question, the deuteration of water may be considered, since the above reaction could also take place with H₂ substituted by HD or D₂, which naturally raises the question of how much HD and D₂ is available on the surface.

In this paper, we aim at estimating the grain surface abundances of H₂, HD, and D₂, by considering molecular hydrogen interactions with the surface of amorphous solid water (ASW). Pure ASW is considered here as a template that mimics the surface of water-dominated icy mantles. To calculate the abundance of H₂ and its isotopologues on such a surface under physical conditions relevant to dark clouds, it is necessary to estimate their

* Present address: Leiden Observatory, Leiden University, PO Box 9513, 2300 RA Leiden, The Netherlands.

population distributions over the surface as a function of the surface temperature and gas-phase densities. In the present case, our calculations incorporate the binding energy distributions of H₂, HD, and D₂ that are fitted to a set of temperature-programmed desorption (TPD) experiments conducted at temperatures of 10–30 K on a porous ASW sample using the experimental set-up FORMOLISM (FORMation of MOlecules in the InterStellar Medium, previously described in, e.g., [Amiaud et al. 2006, 2007, 2008](#)). These values are then incorporated into a toy model that allows us to estimate grain surface abundances of H₂, HD, and D₂.

The article is structured as follows. In Sect. 2 we provide a very short description of the experimental results. In Sect. 3 we present a toy model that allows us to interpret the experimental results and we discuss the validity of this model. Section 4 provides some direct results of this model, that are discussed in an astrophysical context, before giving a closing summary in Sect. 6.

2. Description of desorption

The primary aim of this paper is to obtain the number of hydrogen molecules (and isotopologues) adsorbed onto the interstellar grains. This number is the result of a balance between adsorption and desorption processes.

In the following we present and use results of experiments carried out to study and measure the difference in binding energy of H₂ and its isotopologues (i.e., HD and D₂) on a sample of pure amorphous solid water (ASW) ice. The main experimental results are only briefly reported here. More details in the TPD experiments will be presented in a forthcoming paper. Here we only report on details important for understanding the results.

The experiments were performed in an ultra-high vacuum chamber where a sample of ASW ice was grown on a copper sample. For these experiments we grew 10 mono-layers (1 ML $\equiv 10^{15}$ cm⁻²) of porous ASW ice. Due to the porosity of the ice, the total ice surface is ~ 3.6 times higher than the surface of the copper sample as evaluated in [Amiaud et al. \(2006\)](#). This ice template is believed to be a good template for our purposes (see Sect. 3.2). We performed a set of TPD experiments. It is a technique in which a programmed temperature ramp induces a controlled heating of the surface, while the desorption kinetics of species initially adsorbed on the surface are monitored with a mass spectrometer. These spectra are then analysed in terms of adsorption energy distribution.

A central question arises: Can the time scales used in experiments be translated to astronomical time scales? The answer is yes, because for the description of the experiments we adopt a model, which assumes thermodynamical equilibrium at any moment (see Sect. 3). Therefore, it is not time dependent.

Classically a molecule has a definite adsorption energy E_{ads} , and one can write the desorption flux rate (ϕ_{out}) as

$$\phi_{\text{out}} = \theta A e^{-E_{\text{ads}}/kT} \quad (2)$$

where A is the number of attempts per second of the molecule to desorb, and θ the coverage, i.e., the number of molecules adsorbed per cm². We note that A is inversely proportional to the root of the mass of the species such that $A(\text{H}_2) = A(\text{D}_2) \sqrt{2}$. In the case of an amorphous surface, the adsorption energy is not unique but has to be replaced by a large distribution of energies depending on the coverage $E_{\text{ads}}(\theta)$ (e.g. [Govers et al. 1980](#); [Chang et al. 2005](#); [Hornekær et al. 2005](#); [Amiaud et al. 2006](#);

Table 1. Model fits to experimental results ([Amiaud et al., in prep.](#)), see Eqs. (2) and (3). ΔE_0 is given with respect to $E_0(\text{H}_2)$.

Species	A (s ⁻¹)	E_0 (meV)	ΔE_0 (meV)
H ₂	1.414×10^{13}	71.9	–
HD	1.155×10^{13}	72.1	0.2
D ₂	1.00×10^{13}	74.7	2.8

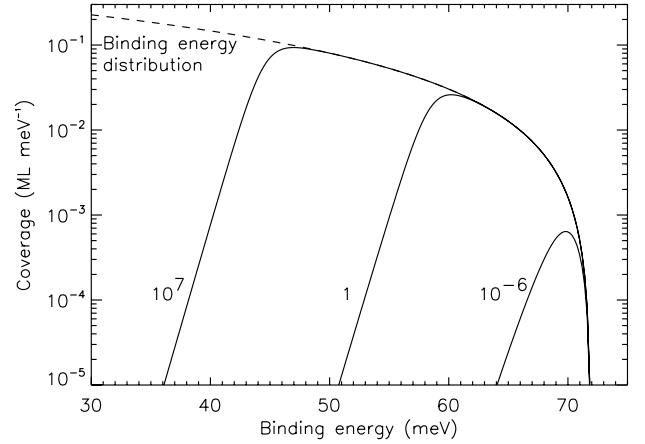


Fig. 1. Adsorption energy distributions of H₂ on a porous ASW ice with a surface at 10 K for three values of desorbing flux equal to accreting fluxes corresponding to number densities in the gas phase at 10 K of $n_{\text{H}_2} = 10^7, 1, 10^{-6}$ cm⁻³ (see text for full description).

[Fillion et al. 2009](#)). We emphasise that the wide binding energy range of these distributions (originating from the amorphous nature of the surface) affects the residence time scales of the molecules on the surface dramatically. Therefore, the amorphous nature of the surface together with small differences in binding energy distributions between isotopologues are governing the amount of species that can accumulate on the surface.

Following [Amiaud et al. \(2006\)](#) we model the distribution of adsorption sites with a polynomial function:

$$g(E) = a(E_0 - E)^b \quad [\text{cm}^{-2} \text{meV}^{-1}]. \quad (3)$$

The parameters a , E_0 , and b are parameters that are determined from fitting the TPD experiments, where also the pre-exponential factor, A , was determined (see Eq. (2)). The two parameters a and b are independent of species, and the best-fit values are $a = 5.86 \times 10^{-4}$ cm⁻² meV^{-2.6} and $b = 1.6$ (without dimension). The fitting of our experimental data to the model using the χ square method shows a very low sensitivity to the A value and consequently a slight change in the E_0 value in the 10^{12} – 10^{13} range, as discussed in [Amiaud et al. \(2006\)](#). As the S/N for D₂ is smaller than for the others isotopes, we have determined 10^{13} for D₂ and calculated the values for HD and H₂ in order to be consistent. The values of A and E_0 are given in Table 1. The difference in the value of E_0 is equal to the difference in zero-point energy, and is also tabulated in Table 1. Using the parameters given in Table 1, one can calculate the desorption rates at a given temperature and given coverage. The problem can be inverted: knowing the desorption rates and coverage, the population distribution on the surface may be derived. Then in the astrophysical context we assume a steady state regime in which the accretion rate (or ϕ_{in}) from the gas phase

is counterbalanced by the desorption rates (or ϕ_{out}) and thereafter constraining the population of adsorption sites.

In Fig. 1 we show schematically such a set of energy occupations of various desorbing fluxes of H₂ at 10 K. The desorbing fluxes are expressed in flux equivalent of n_{H_2} in a dark cloud at 10 K. We see that the denser the cloud is, the more molecules are adsorbed onto the surface, because to compensate for the high incoming flux a greater desorption and therefore a greater coverage is required.

At this point a comparison has to be made with Perets et al. (2007). They performed TPD measurements of ASW ice exposed to atomic D or H beams and to molecular HD or D₂ beams. They extract their parameters using a rate-equations-based model that describes desorption of molecular hydrogen when both atomic and molecular hydrogen are adsorbed on the surface. They find single adsorption energies for HD and D₂ (resp. 68.7 and 72.0 meV) because they have deliberately chosen a low coverage ($\sim 1\%$). Therefore these two energies correspond to the high energy tail of our distribution in Fig. 1. It is noticeable that the difference in E_{ads} for HD and D₂ is in agreement with the results reported here. Nevertheless we want to stress that in this paper we prefer to deal with an energy distribution rather than with unique values of adsorption energies for H₂, HD, and D₂. This is mandatory for the sake of extrapolation to the dense clouds in the interstellar medium (ISM), as in such cases all the species are in competition on the grains ice mantle.

3. Model description and validity

In this section we first describe our model before discussing its validity in an astrochemical context. We have chosen to construct a model based directly on the experimental conditions and results rather than trying to incorporate the present results into a full astrochemical model.

3.1. Model

We have successfully created a model to describe our experimental results (e.g. Amiaud et al. 2006). This model is designed to reproduce our TPD-experiments and we are going here through some of the details.

We start by noting that the change in number of adsorbed molecules, N , on the surface is

$$\frac{dN}{dt} = \phi_{\text{in}} - \phi_{\text{out}} \quad (4)$$

where ϕ_{in} is the rate of adsorption and ϕ_{out} is the rate of desorption. ϕ_{in} may be written as

$$\phi_{\text{in}} = \frac{1}{4} n \bar{v} S \quad (5)$$

where n is the (gas) density, $\bar{v} = \sqrt{8kT/\pi m}$ is the mean velocity at a given temperature, T , and S is the sticking coefficient. We implicitly assume that the gas and surface temperatures are identical and for this reason we set the sticking coefficient equal to unity. The rate of desorption is given by

$$\begin{aligned} \phi_{\text{out}} &= \int_{E_{\text{ads}}} P(E_{\text{ads}}, T, \mu) r(E_{\text{ads}}, T) dE_{\text{ads}} \\ &= \int_{E_{\text{ads}}} P(E_{\text{ads}}, T, \mu) A \exp\left(\frac{-E_{\text{ads}}}{kT}\right) dE_{\text{ads}}. \end{aligned} \quad (6)$$

Here $r(E_{\text{ads}}, T)$ is the desorption rate at a single adsorption site, E_{ads} the adsorption energy and P the population. Because only

one molecule is allowed per adsorption site, the population distribution is given in the Fermi-Dirac formalism (Amiaud et al. 2006) by

$$P(E_{\text{ads}}, T, \mu) = g(E_{\text{ads}}) \left\{ 1 + \exp\left(-\frac{E - \mu}{kT}\right) \right\}^{-1} \quad (7)$$

with μ the Fermi energy or chemical potential.

With respect to describing the population we closely follow the results of Amiaud (2006) and Amiaud et al. (in prep.). They show that the coverage of H₂ on the ice is

$$\begin{aligned} P(E_{\text{H}_2}, T, \mu_{\text{H}_2}) &= a(E_0 - E_{\text{H}_2})^b \times \left\{ 1 + \exp\left(-\frac{E_{\text{H}_2} - \mu_{\text{H}_2}}{kT}\right) \right. \\ &\quad + \exp\left[-\frac{(E_{\text{H}_2} - E_{\text{D}_2}) - (\mu_{\text{H}_2} - \mu_{\text{D}_2})}{kT}\right] \\ &\quad \left. + \exp\left[-\frac{(E_{\text{H}_2} - E_{\text{HD}}) - (\mu_{\text{H}_2} - \mu_{\text{HD}})}{kT}\right] \right\}^{-1} \end{aligned} \quad (8)$$

and similarly for HD and D₂. Here, E_X is the energy of species X , $a = 5.86 \times 10^{-4} \text{ cm}^{-2} \text{ meV}^{-2.6}$, $b = 1.6$ and values for E_0 are given in Table 1. We do not make any assumptions regarding the chemical potential, μ , but calculate it explicitly for each species using the closing relation $\phi_{\text{in}} = \phi_{\text{out}}$ (see below). We now only consider the steady-state solution to Eq. (4), that is $dN/dt = 0$ or $\phi_{\text{in}} = \phi_{\text{out}}$. This allows us to determine the number of adsorbed H₂, HD, and D₂ molecules, N :

$$N = \int_E P(E, T, \mu) dE. \quad (9)$$

3.2. Validity

To use this model in an astrochemical context it is necessary to make a number of assumptions. We go through them here and discuss their validity in detail.

To estimate the gas phase abundance of H₂ and its isotopologues we use the model results of Flower et al. (2004). They modeled the gas phase abundance of compounds containing H and their isotopologues in a time-dependent chemical model. Grains were also included in their model, but only play a role in terms of the total charge distribution. It is important to note that the detailed model results of Flower et al. (2004) only are valid in the absence of heavy elements (see Walmsley et al. 2004, for a full discussion). In our model we do not consider other species than H₂ and its isotopologues, which is in contrast to the real ISM where more than 150 species have been detected so far.

Also, it is necessary to assume that the ice covering dust grains consists of water only, since all experiments are performed on pure water ice. This is again in contrast to real interstellar ices where it is known that ices are composed of several species, e.g., H₂O, CO₂, CO and more complex organic species like CH₃OH (e.g., Gibb et al. 2004). The primary ice component besides H₂O is CO₂ with an abundance of $\sim 10\text{--}50\%$ with respect to H₂O. For our purposes the underlying structure of the ice is not so important as long as the top layer is pure water ice.

Ice morphology and ice template used in the present study are also subject to discussion. The solid icy mantle that covers the grain has an amorphous signature in dense regions (see e.g., Dartois et al. 2002, 2003), but so far the degree of porosity and the thickness is not a direct observational result. The porosity can be very high for an ice grown at 10 K from gas phase (as it is the case in our experiments), but it can easily be reduced

by cosmic rays, UV radiation, thermal processing and possibly chemical processing (Palumbo 2006).

We have demonstrated that there are two types of binding energy distributions, one for the compact amorphous ice and one for the porous amorphous ice. But, as we have shown, the energy distribution of adsorption sites is changing dramatically toward porous distribution as soon as a fraction of a layer of porous ice is deposited on top of a compact amorphous ice (Fillion et al. 2009). Therefore it is highly probable that the correct binding energy distribution of H₂ on icy dust grains is closer to the porous distribution than the compact one. It is classically assumed that the thickness of water ice on grains is about 100 ML in dense clouds (Schutte 1998). Due to processing, the porosity is certainly reduced in comparison to what can be formed in the laboratory. Therefore the 10 ML porous ice sample used in the laboratory would be equivalent to a thicker ice mantle (<100 ML) under astrophysical conditions. We have studied the effect of the change of the porosity in detail, and it does not affect the present study by much. We believe that the ice used in the experiment is a reasonable mean template for the icy, partly processed mantle.

4. Astrophysical implications

By using the above mentioned model, it is possible to extrapolate from laboratory conditions to conditions in the ISM. The main difference in the two scenarios is the much lower molecular flux which is made up for by the much longer time-scales relevant in dark clouds. We therefore adopt the experimental model as a simple toy model of the adsorption and desorption of H₂, HD, and D₂ from an ice-covered grain surface. In doing this we are able to deduce three important results. These are:

- accretion time scales under same assumptions;
- differences in species abundances on the surface of the grain as a function of density assuming initial gas phase conditions as in Flower et al. (2004);
- surface coverage as a function of grain temperature.

Furthermore, we are able to make certain inductions regarding the formation of water, however, this does not arise from an extrapolation of experimental results. In the following we present these results in more detail.

4.1. Accretion time

We first of all want to examine whether our assumption regarding steady-state is realistic compared to the total life-time of a molecular cloud. Statistical equilibrium is reached when a single molecule has sufficient time to explore several adsorption sites on a grain surface through diffusion. Amiaud et al. (2006) already estimated that the average number of sites a molecule can explore is of the order of 10⁹.

We define the steady-state accretion time-scale as

$$\tau_{\text{acc}} = \frac{\theta}{\phi_{\text{in}}}. \quad (10)$$

We show the variation in Fig. 2 as a function of H₂ density at a temperature of 10 K. As expected, the accretion time drops with increasing density. For number densities of 10⁴ cm⁻³ the accretion time scale is ~10³ years in the case of H₂ and HD whereas it is a few times 10³ years for D₂. At very high densities of 10⁷ cm⁻³ the accretion time scale is from a few tens of years to ~10² years. The ratio of accretion time-scales $\tau_{\text{H}_2}:\tau_{\text{HD}}:\tau_{\text{D}_2}$ is

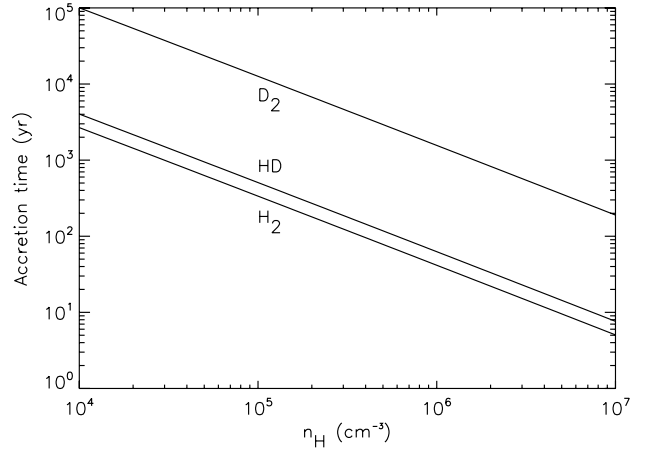


Fig. 2. The accretion time-scale as given in Eq. (10) shown as a function of H₂ number density for H₂, HD, and D₂.

~1:1.5:37.5 independent of the gas phase density of H₂. The reason for this is that both HD and D₂ are more strongly bound to the surface than H₂ and once they are on the surface, they stay there.

In the case of cold dark clouds on their way to undergo star formation, a relevant time-scale and measure for the life-time is the free-fall time, τ_{ff} . For a cloud with a density of 10⁴ cm⁻³ τ_{ff} is of the order of 10⁵ years. As the density increases to 10⁷ cm⁻³ τ_{ff} decreases to ~10⁴ years. In both cases the actual lifetime of the cloud is probably longer due to the effects of both bipolar diffusion and turbulence, two mechanisms that can support a cloud against collapse (e.g., Ballesteros-Paredes et al. 2007), leading to typical cloud lifetimes of ~10⁶ years. Thus, we conclude that our assumption regarding steady-state is valid compared to the total life-time of dark clouds, ~10⁵–10⁶ years. We also note that this result is in agreement with Flower et al. (2004) who find a steady-state time-scale of the order of 10⁵ years, almost independent of number density.

4.2. Surface vs. gas phase abundance

We have calculated the abundance of H₂ and its isotopologues on the surface of dust grain as a function of H₂ gas phase density at a grain and gas temperature of 10 K. Results are shown in Fig. 3.

Because of the higher zero-point energy (2.6 meV higher than HD) D₂ is more tightly bound to the surface and as a result, the abundance of D₂ on the grain surface is ~30 times higher than in the gas phase, when compared to solid and gas phase H₂ respectively. On the other hand, the HD abundance in the gas phase and on the surface are comparable, with a surface abundance that is a few times lower than the D₂ surface abundance. The absolute abundance of D₂ on the surface is ~10⁻⁴ with respect to solid phase H₂. The abundance increases slightly with increasing H₂ number density, when this is in the range of 10⁴–10⁷ cm⁻³. The absolute abundance of HD both on the surface and in the gas phase is a few times 10⁻⁵ with respect to solid and gas phase H₂ respectively. When examining the absolute abundance of H₂ on the surface we find that it is ~2 × 10⁻⁶ with respect to the gas phase abundance. To derive this result, we first calculated the number of grains by assuming a grain/gas

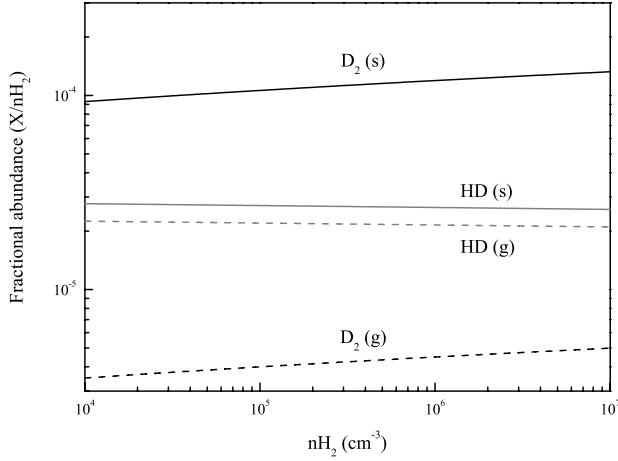


Fig. 3. HD (gray) and D₂ (black) fractional abundances. The gas phase fractional abundances are with respect to gas phase H₂ (g: dashed line) and solid phase fractional abundances are with respect to solid phase H₂ (s: full line). Gas phase abundances are from Flower et al. (2004) and the gas and grain surface temperature are both 10 K.

mass ratio of 0.01, an average grain mass density of 3 g cm⁻³ and that the radius of all grains is 0.1 μm:

$$n_{\text{grain}} = 1.33 \times 10^8 \text{ cm}^{-2} \left(\frac{N_{\text{H}}}{10^{20} \text{ cm}^{-2}} \right) \left(\frac{3 \text{ g cm}^{-3}}{\rho} \right) \left(\frac{0.1 \text{ μm}}{r} \right)^3. \quad (11)$$

We then scaled our experimental fluxes to those of the ISM and from that derived the number of H₂ molecules per cm², which was then converted to total number of H₂ molecules per grain. This implies a density on the surface of ~0.18 compared to H₂O. This is consistent with previous results, where, e.g. Dissly et al. (1994) and Buch & Devlin (1994) find that the surface abundance is ~0.05–0.3 for water ice mixed with H₂. Thus our results show, that in cold, dark molecular clouds, the dominant deuterated species on grains is D₂ and not HD even though HD may be more abundant in the gas phase by a factor ~5 (Flower et al. 2004). We also find that the total amount of D on the grain surface (again, at 10 K and 10⁵ cm⁻³) is of the order of 10⁻⁴ with respect to solid state H₂.

This result is not trivial and deserves a little more attention. The segregation mechanism on the ice is a competition between the three isotopes. For a given site exposed to each of the three isotopes, D₂ has the highest probability to stay, followed by HD and H₂, as can be inferred from the values of adsorption energies. But the probability for an H₂ molecule to stay (meaning that HD and D₂ evaporate) is not zero even if it is low. Therefore, as the number of incoming H₂ molecules is four orders of magnitude greater than for others isotopes, H₂ will succeed in “kicking out” HD quite efficiently because the adsorption energy difference between HD and H₂ is very low (see Table 1). On the other hand, D₂, even if it is the less abundant, has a higher adsorption energy and therefore can compete efficiently with the higher abundance of H₂.

Our model predicts that the abundances of HD and D₂ will be higher with respect to H₂ in the solid phase than with their counterparts in gas phase. However, the absolute H₂ abundance on the grain is so small (~10⁻⁶) that the absolute HD and D₂ solid state abundances with respect to gas phase H₂ is of the order of 10⁻¹⁰, that is, $n_{\text{HD}}^{\text{grain}} \sim n_{\text{D}_2}^{\text{grain}} \sim 10^{-10} n_{\text{H}_2}^{\text{gas}}$.

Lipshat et al. (2004) have made a theoretical study on the formation of H₂, HD, and D₂ on grains. They find an enhanced

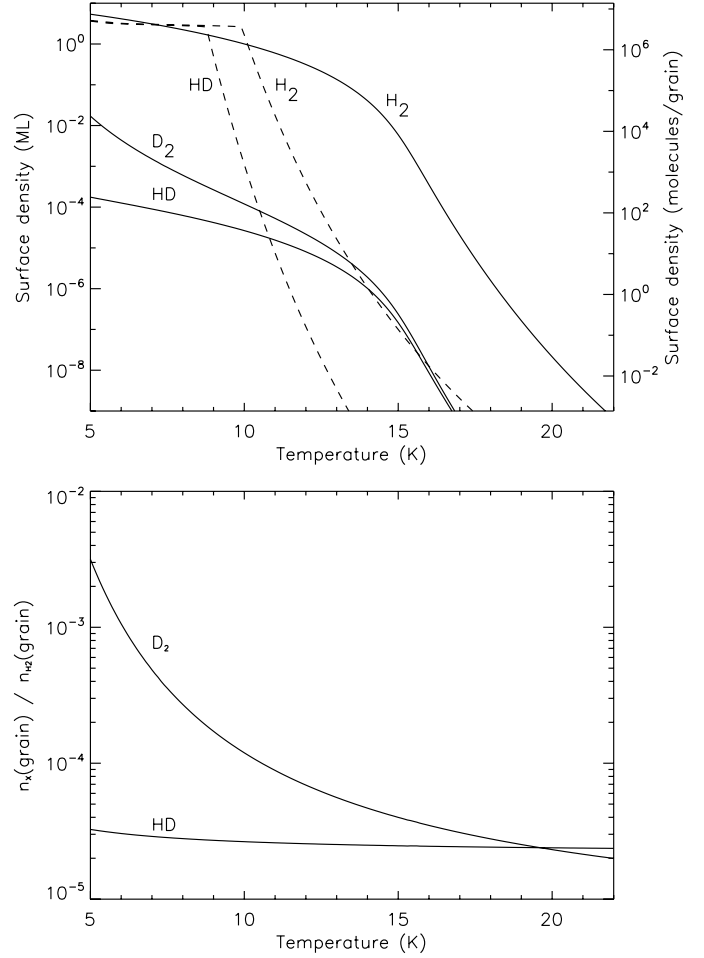


Fig. 4. *Top.* Surface abundance of H₂, HD, and D₂ as a function of temperature for a gas density of 10⁵ cm⁻³ (full lines). We express the surface abundance both in terms of ML but also surface number density for a grain with radius 0.1 μm. For comparison we show the results of Govers et al. (1980) for H₂ and HD (dashed lines). *Bottom.* Fractional abundances of HD and D₂ with respect to H₂ on the surface.

production of HD and D₂ versus H₂ in the 16–20 K range. This is obtained by considering different adsorption energies for H and D atoms. In this range, we find a very low abundance of deuterated molecular hydrogen adsorbed on grain, but a significant amount of H₂ on the grain. This again emphasises the fact that a complete model for molecular hydrogen formation on grains should include the possibility of competition between not only hydrogen atoms and hydrogen molecules but between all the five species (H, D, H₂, HD, and D₂) together on the grain.

4.3. Surface abundance vs. temperature

We show here the results of a calculation of the abundance as a function of temperature for an initial H₂ density of 10⁵ cm⁻³. This is displayed in Fig. 4 both in units of mono-layers (1 ML = 10¹⁵ cm⁻²) and in units of molecules per grain, where we have calculated this for a “standard” grain with radius 0.1 μm. We see that D₂ is more abundant than HD on the surface except at higher temperatures (i.e., >20 K). We also note, that at low temperatures (<6 K) the D₂ abundance comes within 3 orders of magnitude to that of H₂.

We compare our results with the experimental results presented in Govers et al. (1980), noting that these results were

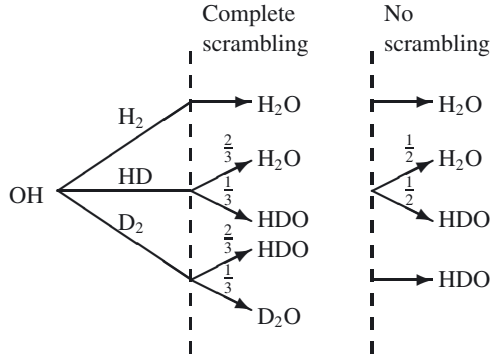


Fig. 5. Water formation involving H₂, HD and D₂ and their branching ratios in the cases where there is complete scrambling in the intermediate H₃O molecule and no scrambling (see reaction 12).

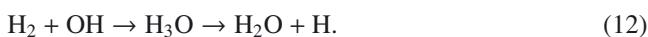
obtained on a non-porous surface. To make a direct comparison we multiplied the coverage values presented in Govers et al. by 3.6. This is shown in Fig. 4. This method does not take competition into account, that is, using this method, it is possible to have one full layer of H₂ adsorbed on the grain as well as one full layer of HD at the same time. This lack of competition is what leads to the break at 9–10 K. Also, we predict a higher abundance at higher temperatures compared to Govers et al. This is a direct result of the higher binding energy.

If we assume a column density towards a dark cloud of $N_{\text{H}} = 10^{20} \text{ cm}^{-2}$, for example, it is possible to convert the local surface density on one grain to a total column density of adsorbed H₂, HD, and D₂ by estimating the total number of grains (see Eq. (11)). This may be compared directly with Fig. 4 to derive a column density of adsorbed H₂ in the case where the local density is 10^5 cm^{-3} . At a temperature of 10 K, we find that it is $N_{\text{H}_2}^{\text{ad}} = 2 \times 10^{14} \text{ cm}^{-2}$, $N_{\text{HD}}^{\text{ad}} = 2 \times 10^{10} \text{ cm}^{-2}$ and $N_{\text{D}_2}^{\text{ad}} = 5 \times 10^9 \text{ cm}^{-2}$. Thus, both adsorbed HD and D₂ are at present not directly detectable in absorption. A detection of solid H₂ is claimed towards the W5 region (Sandford et al. 1993), however this detection still needs confirmation. If true, it would imply an H₂ column density of $\sim 10^{18} \text{ cm}^{-2}$, but this should only be seen as a strict upper limit at present.

5. Case study: water formation

Our model results have so far demonstrated the importance of including the binding energy difference between H₂ and its isotopologues. We emphasise that the results shown here should only give an indication of what can be done with elaborate chemical models that take both gas phase and surface reactions into account.

As an example of application of this result is the deuteration of water. The observed abundance of gas phase deuterated water (HDO) ranges from 10^{-4} to 10^{-2} (Parise et al. 2005). This corroborates a scenario in which water forms on the surface of dust grains through the following surface reaction:



This reaction was originally proposed by Tielens et al. (1983), where it is one among three routes of water formation on dust grains. We only consider this route as it is the only one involving H₂ explicitly and it shows no barrier.

In Fig. 5 we show the possible reactions between H₂, HD or D₂, and OH along with their branching ratios. The branching ratios are determined by assuming that the probability for

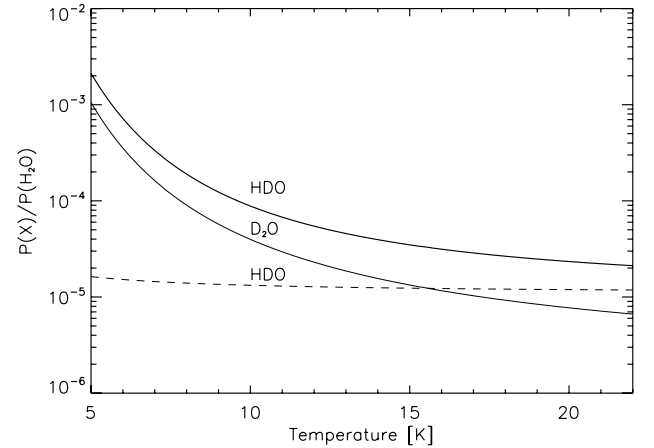


Fig. 6. Water fractionation in the case of complete scrambling (full line) and no scrambling (dashed line). The gas phase density of H₂ is 10^5 cm^{-3} as in Fig. 4.

forming an O–H bond is equal to that of forming an O–D bond. Furthermore we consider both cases with and without complete scrambling of the intermediate H₃O molecule. As an example, we consider the case of OH + HD and assume complete scrambling. The intermediate molecule is H₂DO, i.e., 2/3 of the bonds are with H and 1/3 with D. As a result, the probability of forming H₂O is 2/3 and it is 1/3 for forming HDO.

Since the reaction is without barrier (Tielens et al. 1983), the likelihood that OH will react with H₂, HD, or D₂ depends only on their respective surface coverages (illustrated for the case of complete scrambling only):

$$P(\text{H}_2\text{O}) = k_0 \frac{\theta_{\text{H}_2} + \frac{2}{3}\theta_{\text{HD}}}{\theta_{\text{H}_2} + \theta_{\text{HD}} + \theta_{\text{D}_2}} \quad (13)$$

$$P(\text{HDO}) = k_0 \frac{\frac{1}{3}\theta_{\text{HD}} + \frac{2}{3}\theta_{\text{D}_2}}{\theta_{\text{H}_2} + \theta_{\text{HD}} + \theta_{\text{D}_2}} \quad (14)$$

$$P(\text{D}_2\text{O}) = k_0 \frac{\frac{1}{3}\theta_{\text{D}_2}}{\theta_{\text{H}_2} + \theta_{\text{HD}} + \theta_{\text{D}_2}} \quad (15)$$

where $P(X)$ is the probability of forming X and θ_Y is the surface coverage of species Y . The proportionality constant, k_0 , is identical for all three probabilities (Charnley et al. 1997), again the reason being that the reactions are barrier-less.

If we use the coverages in Fig. 4 it is possible to plot the relative abundance of HDO and D₂O with respect to H₂O as a function of temperature. This is shown in Fig. 6 both in the case of complete and no scrambling. If there is no scrambling, D₂O is not produced unless OH is deuterated, which we do not take into account. We find that typical values of the fractionation are from 10^{-5} – 10^{-4} , implying that this water formation route should contribute with this value to the overall water deuteration. If there is complete scrambling, we find that the abundances of HDO and D₂O are within a factor of 2–3 of each other. We emphasise here, that this is a limiting case and we also stress that the fractionation predicted here is only valid for one route of water formation.

Another way of considering water deuteration is the following. At temperatures lower than ~ 15 K, there will on average always be at least one HD or D₂ molecule present on the grain surface. In the interval of ~ 15 – 19 K, there will be less than one deuterated molecule present per grain, but more than one H₂ molecule. Therefore, at temperatures greater than ~ 15 K,

deuteration of water should not (on average) occur following the above reaction.

Observations of solid phase deuterated water in cold dark clouds places an upper limit of 10^{-3} with respect to H₂ (Parise et al. 2003; Dartois et al. 2003), which is consistent with our results, as long as the water is formed at temperatures greater than ~6 K. It should also be noted, that the above route is not the only one to form water on dust grains (Tielens et al. 1983; Miyauchi et al. 2008; Ioppolo et al. 2008; Dulieu et al. 2010).

6. Summary

In this study, we have used the binding energy distributions valid for H₂, HD, and D₂ adsorbed on a cold porous ASW in order to estimate their abundances on the surface of icy grains mantles under typical dark cloud conditions. The parameters describing the binding energy distributions were obtained from the simulation of a set of TPDs performed between 10 K and 30 K with H₂, HD, and D₂ on a porous 10 ML ASW sample. Our calculation is based upon a model describing the simultaneous interaction of the three species in thermal equilibrium with the surface. The model enables us to extrapolate the experimental results to the astrophysical context, assuming a steady state regime between gas phase accretion and thermal desorption. Our calculation confirms the important role played by the wide range of binding energies and by the small differences in zero-point energy found between the isotopologues. In particular, we have demonstrated that the most abundant deuterated species on a grain surface at 10 K typically is D₂ and not HD, even though the latter is the more abundant gas phase isotopologue.

We have used this to derive certain “order of magnitude” estimates regarding the accretion time-scales and also the surface abundance of these species as functions of both density and temperature. This we have used to estimate water fractionation on grains, as long as it proceeds following one specific formation route.

The results presented here show that a deep understanding of experiments can provide new insights when modeling the interstellar medium. As an example, the difference in binding energy will be one of the main mechanisms responsible for the abundances of deuterated water molecules observed.

Acknowledgements. We acknowledge the support of the French National PCMI programme funded by the CNRS, as well as the strong financial support from

the ANR (Agence Nationale de la Recherche; contract 07-BLAN-0129), the Conseil Régional d’Île de France through a SESAME programme (No. E1315 and I-07-597R) and from the Conseil Général du Val d’Oise. We are indebted to H. Cuppen for very fruitful discussions.

References

- Amiaud, L. 2006, Ph.D. Thesis, Université de Cergy-Pontoise, <http://tel.archives-ouvertes.fr/tel-00124797/en/>
- Amiaud, L., Fillion, J.-H., Baouche, S., et al. 2006, *J. Chem. Phys.*, 124, 094702
- Amiaud, L., Dulieu, F., Fillion, J.-H., Momeni, A., & Lemaire, J. L. 2007, *J. Chem. Phys.*, 127, 144709
- Amiaud, L., Momeni, A., Dulieu, F., et al. 2008, *Phys. Rev. Lett.*, 100, 056101
- Ballesteros-Paredes, J., Klessen, R. S., Mac Low, M.-M., & Vazquez-Semadeni, E. 2007, in *Protostars and Planets V*, ed. B. Reipurth, D. Jewitt, & K. Keil, 63
- Buch, V., & Devlin, J. P. 1994, *ApJ*, 431, L135
- Chang, Q., Cuppen, H., & Herbst, E. 2005, *A&A*, 434, 599
- Charnley, S. B., Tielens, A. G. G. M., & Rodgers, S. D. 1997, *ApJ*, 482, L203
- Congiu, E., Matar, E., Kristensen, L. E., Dulieu, F., & Lemaire, J.-L. 2009, *MNRAS*, 397, 96
- Cuppen, H. M., & Herbst, E. 2007, *ApJ*, 668, 294
- Dartois, E., d’Hendecourt, L., Thi, W., Pontoppidan, K. M., & van Dishoeck, E. F. 2002, *A&A*, 394, 1057
- Dartois, E., Thi, W.-F., Geballe, T. R., et al. 2003, *A&A*, 399, 1009
- Dissly, R. W., Allen, M., & Anicich, V. G. 1994, *ApJ*, 435, 685
- Dulieu, F., Amiaud, L., Congiu, E., et al. 2010, *A&A*, 512, 30
- Fillion, J.-H., Amiaud, L., Congiu, E., et al. 2009, *Phys. Chem. Chem. Phys.*, 11, 4396
- Flower, D. R., Pineau des Forêts, G., & Walmsley, C. M. 2004, *A&A*, 427, 887
- Gibb, E. L., Whittet, D. C. B., Boogert, A. C. A., & Tielens, A. G. G. M. 2004, *ApJS*, 151, 35
- Govers, T., Mattered, L., & Scoles, G. 1980, *J. Chem. Phys.*, 72, 5446
- Hornekær, L., Baurichter, A., Petrunin, V. V., Field, D., & Luntz, A. C. 2003, *Science*, 302, 1943
- Hornekær, L., Baurichter, A., Petrunin, V. V., et al. 2005, *J. Chem. Phys.*, 122, 124701
- Ioppolo, S., Cuppen, H. M., Romanzin, C., van Dishoeck, E. F., & Linnartz, H. 2008, *ApJ*, 686, 1474
- Lipshtat, A., Biham, O., & Herbst, E. 2004, *MNRAS*, 348, 1055
- Miyauchi, N., Hidaka, H., Chigai, T., et al. 2008, *Chem. Phys. Lett.*, 456, 27
- Palumbo, M. E. 2006, *A&A*, 453, 903
- Parise, B., Simon, T., Caux, E., et al. 2003, *A&A*, 410, 897
- Parise, B., Caux, E., Castets, A., et al. 2005, *A&A*, 431, 547
- Perets, H.B., Lederhandler, A., Biham, O., et al. 2007, *A&A*, 661, 163
- Sandford, S. A., Allamandola, L. J., & Geballe, T. R. 1993, *Science*, 262, 400
- Schutte, W. A. 1998, in *Astrophysics and Space Science Library*, ed. P. Ehrenfreund, C. Krafft, H. Kochan, & V. Pirronello, 236, 69
- Tielens, A. G. G. M., Hagen, W., & Greenberg, J. M. 1983, *J. Phys. Chem.*, 87, 4220
- Walmsley, C. M., Flower, D. R., & Pineau des Forêts, G. 2004, *A&A*, 418, 1035